

STUDY ON MECHANICAL PROPERTIES AND ACOUSTIC EMISSION RESPONSE OF DEEP GRANITE UNDER HYDRO-MECHANICAL COUPLING

by

**Qi-Jun HAO^{a,b}, Zhao-Peng ZHANG^{c,d*}, Xin-Zhong WANG^{a,b}, Ru ZHANG^{a,b},
An-Lin ZHANG^{a,b}, Lan-Bin ZHANG^{a,b}, and Chen-Di LOU^{a,b}**

^aState Key Laboratory of Hydraulics and Mountain River Engineering, Sichuan University, Chengdu, China

^bCollege of Water Resource and Hydropower, Sichuan University, Chengdu, China

^cCollege of Architecture and Environment, Sichuan University, Chengdu, China

^dMOE Key Laboratory of Deep Earth Science and Engineering, Sichuan University, Chengdu, China

Original scientific paper

<https://doi.org/10.2298/TSCI2301631H>

The study on the mechanical response of deep rock under hydromechanical couplings condition can guide the safe excavation and stability evaluation of deep tunnel engineering. The effects of monotonic loading and cyclic loading on the mechanical properties of granite under 5 MPa pore water pressure and 10 MPa confining pressure were studied by laboratory tests. Before the peak stress, the permeability under monotonic loading was significantly higher than that under cyclic loading, and the permeability under cyclic loading increased sharply after the peak stress. There were two active periods of the acoustic emission energy before peak stress under monotonic loading, but it was always in relative quiet period under cyclic loading before peak stress. Based on the energy theory, the energy evolution of granite was discussed. The dissipation energy can better reflect the effect of loading mode on the energy evolution.

Key words: hydraulic coupling, granite, acoustic emission, energy dissipation

Introduction

With the development of deep geotechnical engineering and underground space utilization, the rock mass of underground engineering is always faced with the environment of high pore water pressure, which gradually becomes an important factor of safe excavation and operation of deep engineering. For example, the maximum external water pressure on the structure of the Jinping-II Hydropower Station is 10.22 MPa, and the maximum single point water output is 7.3 m³/s [1]. According to the drilling data, there exist high pore water pressure at several boreholes in deep tunnel in Zheduo mountain, and the construction of the tunnel will face the risk of water bursting [2, 3]. At the same time, a large number of research have shown that the mechanical properties of rock itself will change significantly under the action of hydraulic coupling [4-7]. Therefore, the study of rock mechanical characteristics under hydraulic

*Corresponding author, e-mail: zhangzp@scu.edu.cn

coupling is of great significance for deep geotechnical engineering and underground space utilization.

In the excavation of deep geotechnical engineering, the surrounding rock mechanics environment is often affected by the excavation. Due to the influence of different excavation methods, the rock mass is repeatedly in the process of stress adjustment with the increase of circumferential stress and the unloading of radial stress. Therefore, it is of great practical significance to study the effect of cyclic loading on the mechanical properties of rock. Through a series of monotonic and cyclic loading experiments on granite, Xiong *et al.* [8] found that with the continuous accumulation of damage, both the peak stress and the crack initiation threshold decreased. Zhang *et al.* [9] conducted cyclic loading test on granite under hydromechanical coupling condition, and pointed out that cyclic loading has important influence on permeability and energy dissipation of granite. Zhang *et al.* [10] discussed the permeability of granite under cyclic loading, and discovered that the permeability during unloading is less than that during loading. Ning *et al.* [11] investigated the mechanical properties and permeability of granite under cyclic loading combined with hydraulic coupling tests, and discovered that crack propagation, damage evolution and permeability evolution are closely related. Many scholars have paid much attention to the mechanical properties and seepage characteristics of rock under cyclic loading [12-14], but the effect of different stress paths on the mechanical response of rock under hydraulic coupling condition and its mechanism are not clear, more research is necessary.

In the process of rock deformation and failure, there is an evolution process of development and expansion of the internal micro-cracks, which is accompanied by acoustic emission (AE) [15-17]. The AE, as a non-destructive monitoring method of rock internal damage, can well reflect the evolution of rock internal cracks and reveal the mechanism behind the mechanical response. Therefore, the monotonic loading and cyclic loading tests with pore water pressure of 5 MPa and confining pressure of 10 MPa are designed for deep granite, the effects of different loading modes on the mechanical parameters, permeability, AE characteristics and energy evolution of granite were investigated.

Hydraulic coupling test of deep granite

Description of rock samples and testing facilities

The granite samples used in this test are taken from the No. 2 borehole of Zheduo Mountain 1# Tunnel, China, and the depth is 771~798 m. According to ISRM's suggestion, ϕ 50 mm \times L 100 mm cylindrical standard granite samples were made by core sampling, cutting and grinding. The specimen has a smooth surface and a compact structure, fig. 1(a). The hydraulic coupling test is conducted by MTS815 rock mechanics test system, fig. 1(b), which is used for the hydraulic coupling triaxial test with a maximum axial load of 4600 kN, a maximum confining pressure of 140 MPa and a maximum pore pressure of 140 MPa. The AE test is conducted by using PCI-II AE system, and the real-time acquisition and storage of AE signal time-space distribution and wave velocity are realized by using eight AE sensors. In order to reduce the influence of noise and attenuation of acoustic wave on the test results, the threshold of AE signal acquisition is set to 40dB.

In the process of test preparation, the confining pressure is first applied to the target confining pressure of 10 MPa at a rate of 4 MPa per minute, and the pore water pressure is applied to the target value of 5 MPa at a rate of 4 MPa per minute after the confining pressure is stabilized. In order to compare and analyze the effect of engineering disturbance on the me-

chanical properties of granite, a group of hydraulic coupling cyclic loading tests were designed. The stress path of cyclic loading test is shown in fig. 1(c). After loading to 50 MPa at a rate of 3 MPa per minute, it enters the stress maintenance stage. In each subsequent loading process, the target stress increases by 50 MPa each time until the last residual stress stage. It should be noted that in the monotonic loading test, stress shall be maintained for every 50 MPa increase, and permeability shall be measured once.

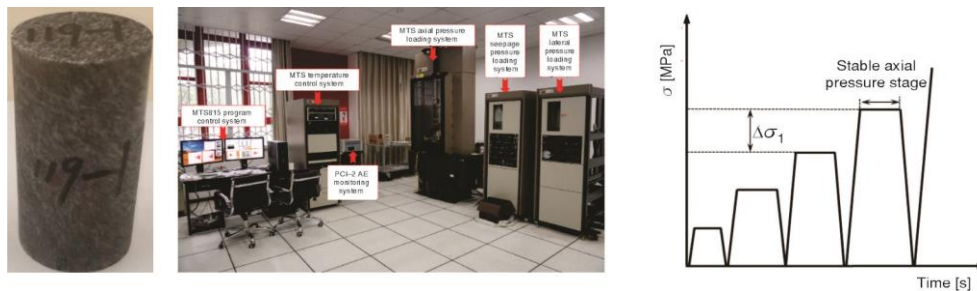


Figure 1. Granite sample of THM coupling test; (a) granite specimen, (b) MTS815 rock mechanics test system, and (c) stress path of cyclic loading test

Mechanical properties and AE characteristics of deep granite under hydro-mechanical coupling

Stress-strain curves

The stress-strain curves of granite under monotonic loading (ML) and cyclic loading (CL) are shown in fig. 2. In order to better analyze the mechanical properties of granite under loading, the stress-strain curves are marked by several characteristic stresses. In monotonic loading, fig. 2(a), the initiation stress, σ_{ci} , is determined by the transverse stress difference method (ΔLSR) proposed by Zhao *et al.* [18] and Nicksiar [19], and the damage stress, σ_{cd} , is the stress corresponding to the maximum volume strain. In cyclic loading, the inflexion of the first rise curve of axial strain-crack volumetric strain under cyclic loading and unloading is taken as crack initiation stress, σ_{ci} , and the maximum value of volumetric strain is damage stress, σ_{cd} [20].

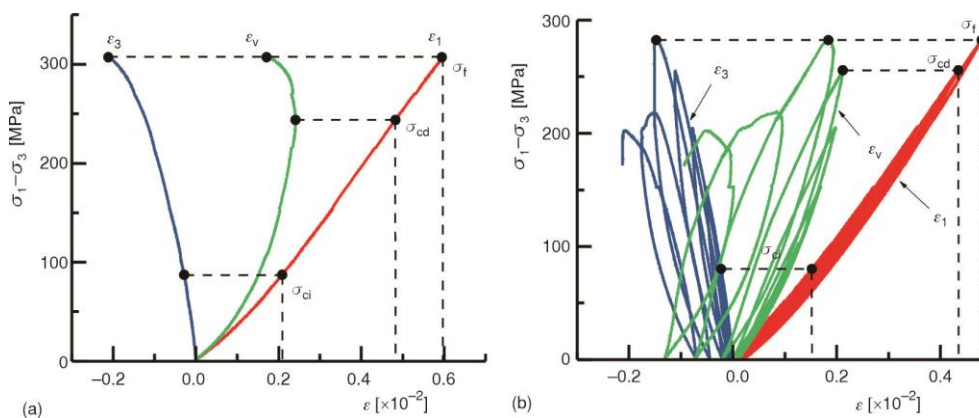


Figure 2. Stress-strain curves of granite under hydromechanical coupling; (a) $\sigma_3 = 10$ MPa, $P_w = 5$ MPa, ML and (b) $\sigma_3 = 10$ MPa, $P_w = 5$ MPa, CL

In fig. 2(a), when the stress value is less than the initial fracture stress, σ_{ci} , the axial stress-strain curve has obvious non-linear characteristics due to the closure of the primary fracture and the compaction of the colloidal particles. During cyclic loading, the stress-strain curve before crack initiation undergoes a stress cycle, and the compaction effect on granite results in that its non-linear characteristics is less obvious than that of monotonic loading. When the stress value is between σ_{ci} and σ_{cd} , the granite enters the crack initiation stage, the axial stress-axial strain curve increases linearly under monotonic loading, and the increase of volume strain slows down until it reaches the maximum. Meanwhile, the granite undergoes four stress cycles during cyclic loading, the area of stress hysteresis loop increases gradually, which indicates that the cumulative damage of granite increases gradually.

Permeability of granite

The well-known permeability is given:

$$K = \frac{\nu\beta VL_s \ln\left(\frac{\Delta P_i}{\Delta P_f}\right)}{2\Delta t A_s} \quad (1)$$

where ν is the viscosity of the pore fluid (we take 0.01), β – the compressibility of the pore fluid (we take $4.53 \cdot 10^{-10}$), V – the volume of the pressure-stabilizing vessel (we take 319), L_s – the height of the pattern, ΔP_i – the initial pressure difference, ΔP_f – the final pressure difference, Δt – the duration, and A_s – the cross-sectional area of the rock.

The permeability is shown in fig. 3. The permeability of the first two stress cycles during cyclic loading does not meet the measurement criteria and is therefore not shown in fig. 3. Under monotonic loading, the permeability shows a trend of decreasing at first and then increasing gradually, and it reaches minimum when the stress level is 50%. At the stress level of 33~50%, the decrease of permeability is due to the closure of primary fractures of granite, which results in the closure of some microscopic seepage channels. During cyclic loading, the permeability increases gradually. When the stress level is 87%, the permeability is $1.187 \cdot 10^{-15} \text{ m}^2$. At the end of the test, the permeability reaches $2.566 \cdot 10^{-14} \text{ m}^2$, which increases 21.62 times. This is due to the formation of macro-cracks in granite during the post-peak stress stage, and the increase of friction damage of macroscopic crack surface and the widening of seepage passage under loading and unloading. In addition, the permeability under cyclic loading is significantly lower than that under monotonic loading before the peak stress, which reflects the effect of cyclic loading on granite fracture.

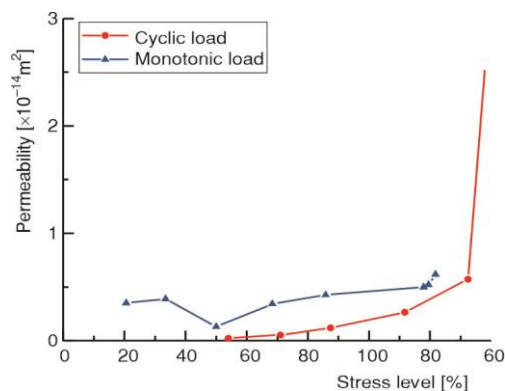


Figure 3. Permeability-stress level curves of granite under hydro-mechanical coupling

The AE energy evolution

The AE energy represents the area under the envelope of AE signal, and many researches have proved that the AE energy reflects the development and propagation of rock

micro-cracks. Figure 4 shows the AE energy-time curve and stress-time curve of granite under monotonic and cyclic loading. In monotonic loading, fig. 4(a), when the loading time is less than 2456 seconds, the granite is in the elastic stage and the fracture initiation stage, and AE energy is in the quiescent stage. The first peak-value of AE energy is $2.22 \cdot 10^{-19}$ J when the stress increases to near the damage stress. When the stress is greater than σ_{cd} the AE energy enter an active period, and the second peak value of $5.80 \cdot 10^{-19}$ J appears at the peak stress σ_f . In the post-peak phase, AE energy are also active due to stress adjustment and friction between the main crack surfaces. In cyclic loading, fig. 4(b), when the stress is less than σ_{cd} , the AE energy is in the initial quiescent period, and there is no obvious AE energy due to stress loading and unloading. When the stress is greater than σ_{cd} , the AE energy gradually enters the active period, and the first peak value of $1.40 \cdot 10^{-19}$ J appears near the peak stress.

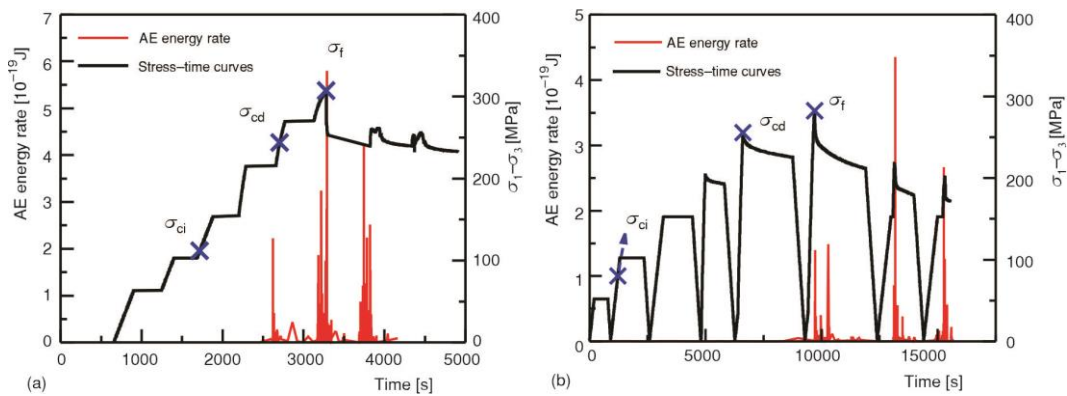


Figure 4. The AE energy-time curve and stress-time curve of granite under hydro-mechanical coupling; (a) $\sigma_3 = 10$ MPa, $P_w = 5$ MPa, ML, (b) $\sigma_3 = 10$ MPa, $P_w = 5$ MPa, CL

Energy and damage evolution

Energy theory

The energy input into the rock under load is partly stored in the rock by elastic strain energy and partly dissipated by crack development, propagation and penetration. If the unit volume of granite unit is assumed to have no energy exchange with the outside world, no energy loss such as AE and radiation energy, *etc.* There is:

$$U = U_e + U_d \quad (2)$$

where U is the total energy, U_e – the elastic strain energy, and U_d – the dissipative energy.

As shown in fig. 5, under a single OA loading-AB unloading cycle, the area surrounded by OAC represents the total energy U_i of a cycle. The area surrounded by OAB represents the dissipated energy U_i^d of a cycle the area around ABC represents the elastic strain energy of a cycle. Here, we have:

$$U_i = \int_0^{\varepsilon_1^i} \sigma d\varepsilon \quad (3)$$

$$U_i^e = \int_{\varepsilon_1^i}^{\varepsilon_1^{i+1}} \sigma d\varepsilon \quad (4)$$

and

$$U_i^d = U_i + U_i^e \quad (5)$$

where $\varepsilon_{1,i}^d$ is the cyclic axial plastic strain and is $\varepsilon_{1,i}^e$ the cyclic axial elastic strain.

Under monotonic loading, there exists $U_d = U - U_e$ where:

$$U = \int_0^{\varepsilon_1} \sigma_1 d\varepsilon_1 + \int_0^{\varepsilon_2} \sigma_2 d\varepsilon_2 + \int_0^{\varepsilon_3} \sigma_3 d\varepsilon_3 \quad (6)$$

and

$$U_e = \frac{1}{2E_u} [\sigma_1^2 + \sigma_2^2 + \sigma_3^2 - 2\nu_u (\sigma_1\sigma_2 + \sigma_2\sigma_3 + \sigma_1\sigma_3)] \quad (7)$$

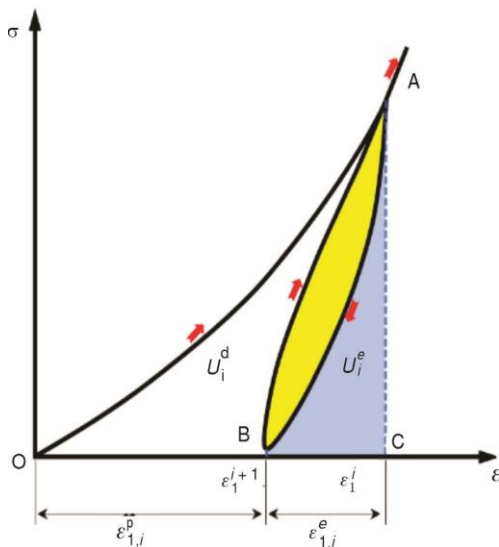


Figure 5. Calculation method for elastic energy and dissipated energy in a rock unit

There are general cases of the stress and strain suggested in [21]. The unloading elastic modulus E_u and unloading Poisson's ratio ν_u can be replaced by the elastic modulus and Poisson's ratio in the elastic stage respectively.

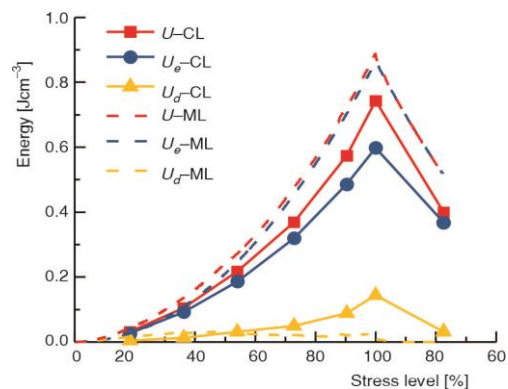


Figure 6. Energy evolution of granite

Energy evolution analysis

The stress level calculated by the ratio of the real-time stress to the peak stress is taken as the abscissa, and the elastic strain energy, U_e , dissipated energy, U_d , and total strain energy, U , under monotonic loading and cyclic loading is taken as the ordinate, fig. 6. It's concerned that the stress level below 100% in the right half of the abscissa represents the post-peak phase. Under cyclic loading, U_e , U_d , and U increase non-linearly with the increase of stress level before the peak stress, and decrease obviously at the post-peak stress stage. Under monotonic loading, before the peak stress, U and U_e increase with the increase of stress level, while U_d increases first and then decreases. Comparing the energy evolution under the two conditions, it can be found that the significant difference is reflected in the dissipative energy U_d . Under monotonic loading, U_d reaches a peak value of 0.0327 J/cm^3 at the stress level of 50% before the peak, and then decreases gradually with the test. Under cyclic loading, U_d reaches a peak value of 0.144 J/cm^3 at the peak stress, and is less at the early stage of the test. At the pre-peak stress level of 54%, the dissipation energy increases faster than that under monotonic loading.

These differences result from the different loading modes, in the previous process, due to the compression effect of cyclic loading, energy dissipation is smaller. However, near the peak stress stage, the damage degree of granite will increase under cyclic loading, more micro-cracks will develop and more energy will be consumed during loading.

Conclusion

Through the monotonic loading and cyclic loading tests of granite under 5 MPa pore water pressure and 10 MPa confining pressure, the effects of different loading modes on the mechanical parameters, AE energy evolution of granite under hydromechanical coupling were investigated. The peak strength of granite under cyclic loading is smaller than that under monotonic loading. The permeability of granite under monotonic loading before peak stress is greater than that under cyclic loading, while the permeability of granite under cyclic loading after peak stress increases greatly. The AE energy shows that the fracture evolution of granite under monotonic loading is more active than that under cyclic loading. Based on the energy theory, the energy evolution of granite under two loading modes is discussed, and it is found that dissipative energy is the key to the evolution of reaction cracks.

Acknowledgment

The study was financially supported by the National Natural Science Foundation of China under Grant No. 52125402, and the Natural Science Foundation of Sichuan Province, China under Grant No. 2022NSFSC0005.

Nomenclature

| | |
|--------------|---|
| A_s | – sample cross-sectional area, [cm ²] |
| E_u | – unloading elastic modulus, [GPa] |
| L_s | – sample height, [mm] |
| P_w | – pore water pressure, [MPa] |
| ΔP_i | – initial pressure difference, [MPa] |
| ΔP_f | – final pressure difference, [MPa] |
| Δt | – duration, [s] |
| U | – total strain energy, [Jcm ⁻³] |
| U_d | – dissipated energy, [Jcm ⁻³] |
| U_e | – elastic strain energy, [Jcm ⁻³] |
| V | – pressure-stabilizing vessel volume [cm ³] |
| ν_u | – unloading Poisson's ratio, [–] |

Greek symbols

| | |
|-----------------------|---|
| β | – pore fluid compressibility, [MPa] |
| $\varepsilon_{1,i}^e$ | – axial elastic strain of a cyclic, [–] |
| $\varepsilon_{1,i}^d$ | – axial plastic strain of a cyclic, [–] |
| σ_1 | – axial stress, [MPa] |
| σ_3 | – confining pressure, [MPa] |
| σ_f | – peak stress, [MPa] |
| σ_{cd} | – damage stress, [MPa] |
| σ_{ci} | – initiation stress, [MPa] |
| $\Delta\sigma$ | – stress increment, [MPa] |
| ν | – pore fluid viscosity, [Pa s] |
| ϕ | – sample diameter, [mm] |

References

- [1] Zhang, C., *et al.*, Key Technologies and Risk Management of Deep Tunnel Construction at Jinping II Hydropower Station, *Journal of Rock Mechanics and Geotechnical Engineering*, 8 (2016), 4, pp. 499-512
- [2] Xu, Z., *et al.*, Detection of Water-Rich Fractured Rock Masses along Proposed Railway Tunnel Routes Using Three-Dimensional Aero-Electromagnetic Methods, *IOP Conference Series: Earth and Environmental Science*, 570 (2020), 10, 052041
- [3] Xu, M., *et al.*, Major Engineering Hydrogeological Problems along the Ya'an-Linzi Section of the Sichuan-Tibet Railway, *Hydrogeology & Engineering Geology*, 48 (2021), 5, pp. 13-22
- [4] Wang, Z. C., *et al.*, Hydro-Geochemical Analysis of the Interplay between the Groundwater, Host Rock and Water Curtain System for an Underground Oil Storage Facility, *Tunnelling and Underground Space Technology*, 71 (2018), 1, pp. 466-477
- [5] Zhang, B., *et al.*, Assessing the Water-Sealed Safety of an Operating Underground Crude Oil Storage Adjacent to a New Similar Cavern - a Case Study in China, *Engineering Geology*, 249 (2019), 1, pp. 257-272

- [6] Gao, H., et al., Experimental Study on Influence of Intermediate Principal Stress on the Permeability of Sandstone, *Transport in Porous Media*, 135 (2020), 3, pp. 753-778
- [7] Ai, T., et al., Changes in the Structure and Mechanical Properties of a Typical Coal Induced by Water Immersion, *International Journal of Rock Mechanics and Mining Sciences*, 138 (2021), 1, 104597
- [8] Xiong, L., et al., Mechanical Behavior of a Granite from Wuyi Mountain: Insights from Strain-Based Approaches, *Rock Mechanics and Rock Engineering*, 52 (2018), 3, pp. 719-736
- [9] Zhang, C. H., et al., Hydraulic Properties and Energy Dissipation of Deep Hard Rock under H-M Coupling and Cycling Loads, *Thermal Science*, 23 (2019), Suppl. 3, pp. S935-S942
- [10] Zhang, H. Y., et al., Effect of Stress Induced Damage on Gas Permeability of Beishan Granite, *European Journal of Environmental and Civil Engineering*, 2020 (2020), 7, 1796818
- [11] Ning, Z. X., et al., Damage Characteristics of Granite under Hydraulic and Cyclic Loading–Unloading Coupling Condition, *Rock Mechanics and Rock Engineering*, 55 (2022), 3, pp. 1393-1410
- [12] Zhou, Z. L., et al., Permeability Evolution of Fractured Rock Subjected to Cyclic Axial Load Conditions, *Geofluids*, 2020 (2020), 1, 4342514
- [13] Zhang, X. B., et al., Experimental Study on Seepage Properties of Postpeak Fractured Rocks under Cyclic Loading–Unloading Confining Stress and Axial Stress, *Geofluids*, 2021 (2021), 1, 6629835
- [14] Zhou, Y., et al., Fatigue Damage Mechanism and Deformation Behaviour of Granite under Ultrahigh-Frequency Cyclic Loading Conditions, *Rock Mechanics and Rock Engineering*, 54 (2021), 9, pp. 4723-4739
- [15] Lu, H., et al., Damage Characterization of Shale under Uniaxial Compression by Acoustic Emission Monitoring, *Frontiers of Earth Science*, 15 (2021), 4, pp. 817-830
- [16] Wang, X. Z., et al., Mechanical Properties and Acoustic Emission Characteristics of Granite under Thermo-Hydro-Mechanical Coupling, *Thermal Science*, 25 (2021), 6B, pp. 4585-4596
- [17] Zha, E. S., et al., Long-Term Mechanical and Acoustic Emission Characteristics of Creep in Deeply Buried Jinping Marble Considering Excavation Disturbance, *International Journal of Rock Mechanics and Mining Sciences*, 139 (2021), 3, 104603
- [18] Zhao, X. G., et al., Objective Determination of Crack Initiation Stress of Brittle Rocks under Compression Using AE Measurement, *Rock Mechanics and Rock Engineering*, 48 (2015), 6, pp. 2473-2484
- [19] Nicksiar, M., Evaluation of Methods for Determining Crack Initiation in Compression Tests on Low-Porosity Rocks, *Rock Mechanics and Rock Engineering*, 45 (2012), 4, pp. 607-617
- [20] Zhao, J., et al., Experimental Study of Deformation and Failure Characteristics of Deeply-Buried Hard Rock under Triaxial and Cyclic Loading and Unloading Stress Paths (in Chinese), *Rock and Soil Mechanics*, 41 (2020), 5, pp. 1521-1530
- [21] Yang, X. J., et al., On the Theory of the Fractal Scaling-law Elasticity, *Meccanica*, 57 (2022), 4, pp. 943-955